

# Nonlinear Phase Macromodel Based Simulation/Design of PLLs with Superharmonically Locked Dividers

Shweta Srivastava, Xiaolue Lai and Jaijeet Roychowdhury  
 Department of Electrical and Computer Engineering, University of Minnesota  
 Emails: {shwetasa, laixl, jr}@umn.edu

**Abstract**—We present a novel nonlinear phase macromodel based technique for quickly and accurately predicting superharmonic injection locking (SHIL) in injection-locked frequency dividing (ILFD) oscillators and PLLs. Our approach is useful for both hand analysis and fast/accurate simulation. We derive an analytical phase slope and periodicity based criterion for detecting SHIL from macromodel simulations and present an insightful way of understanding SHIL phenomena using phase macromodels. We present detailed examples of the new technique and validate our results against full SPICE-level simulation, obtaining speedups of 150–200 $\times$ .

## I. INTRODUCTION

PLLs are heavily used in electronics, communication and instrumentation. They are used in clock generators, RF and wireless transceivers, frequency synthesizer, optical fiber receivers, jitter/skew reduction circuits, *etc.*. In many RF applications, PLLs are used for frequency synthesis, *i.e.*, for generating a programmable output frequency that is, *e.g.*, a multiple of a high-quality low frequency signal [1]. Standard architectures for PLL synthesizers involve placing a frequency divider within the PLL's feedback loop, as shown in Fig. 1. The most common approach to frequency division is to use digital counters [2]; however, digital dividers tend to be more difficult to design at very high frequencies, as well as to consume more power, than analog alternatives [3], [4]. In this context, there has been considerable recent interest [5], [6] in the use of *injection-locked frequency dividers* (ILFD) for frequency division, due to their design simplicity and their property of maximizing speed/power performance in a given technology.

Oscillators exhibit frequency division via *superharmonic injection locking* (SHIL), a special form of a universal phenomenon known as *injection locking* (IL) in oscillators. IL refers to the fact that when an oscillator is disturbed by an external signal, it can, under appropriate conditions, change its oscillation frequency to exactly match the frequency of the disturbance; SHIL refers to the fact that an oscillator's frequency can adjust itself so that the disturbing frequency becomes an *exact integer multiple* of the new oscillation frequency — thereby effectively dividing the disturbing frequency. In other words, if the oscillator's free running frequency is  $f_0$  and it is disturbed by a signal of frequency  $f_1$ , it can “lose” its original frequency  $f_0$  and start oscillating at frequency  $f_1/M$  (where  $M$  is an integer). Typically, this occurs only if  $f_1/M$  and  $f_0$  are close to each other.

In spite of their performance advantages and small circuit sizes compared to digital dividers, ILFDs can be challenging to design because of the complex nonlinear dynamics of oscillators in general and the SHIL phenomenon in particular. Prior attempts to understand and predict IL and SHIL from the design perspective [7]–[9] have tended to rely largely on linearized analysis. While aspects of linear analysis are useful, it leads to an incomplete understanding of IL phenomena and provides only approximate predictive power. The work of Rategh and Lee [6] recognized the crucial rôle of nonlinearities in IL/SHIL and used polynomial approximations for circuit nonlinearities in their analysis. It should be noted, however, that polynomial approximations are not very well suited for strong nonlinearities (such as those arising in, *e.g.*, diodes, BJTs and MOSFETs).

From a simulation and numerical analysis standpoint, oscillators and IL/SHIL also present unique challenges. The standard approach of using transient simulation to predict IL/SHIL is often extremely inefficient and also inaccurate; this is because transient simulation of oscillators faces unique numerical challenges that stem fundamentally from their autonomous nature [10]–[13]. In practice, oscillator transients can last thousands of cycles, thereby exacerbating computation and inaccuracy problems. Another issue is that it is often

difficult to determine by observation of transient waveforms small frequency differences between the disturbing signal's frequency and the oscillator's perturbed frequency.

In this paper, we present a new technique for accurate and efficient prediction of SHIL that is useful for both hand analysis and for fast/accurate simulation. The technique is based on the automated extraction and use of *nonlinear phase macromodels* of oscillators [13]–[15]. In recent years, such nonlinear phase macromodels have been shown to be effective for predicting a variety of oscillator and PLL phenomena [12]–[14], including (same-harmonic) IL, phase noise, jitter from power/ground interference, PLL lock/capture dynamics, cycle slipping, *etc.*. In this paper, we extend the applicability of nonlinear phase macromodels to SHIL in ILFDs and ILFD-based PLLs, as well.

We first analyze the nonlinear phase macromodel (which uses a quantity called the Perturbation Projection Vector or PPV [14]) “by hand” to provide insights into how SHIL occurs. In the process, we clarify how nonlinearity is critical to the SHIL process. Using this analysis, we also obtain simple mathematical criteria that enable us to determine whether a simulation (also based on the nonlinear PPV macromodel) is predicting SHIL or not.

We then apply the PPV macromodel to simulate SHIL, first in a standalone LC oscillator acting as an ILFD, then within a PLL (containing two oscillators, the VCO and the ILFD). We demonstrate the usefulness of the nonlinear PPV macromodel in predicting the correct behaviour of the system in all cases — whether or not ILFD occurs (using the criterion noted above). We validate the new technique via comparisons against careful and detailed SPICE-level transient simulations of the original circuits. Using the new technique results in speedups of 2–3 orders of magnitude.

Compared to prior approaches for the analysis and simulation of oscillatory and PLL systems with ILFDs, our technique has a number of other advantages as well. The technique is generically applicable to any kind of oscillator and is not limited to, *e.g.*, simple LC oscillators. Indeed, the PPV macromodel is extracted in a push of a button — *i.e.*, via numerical algorithm — from a full SPICE-level circuit of the ILFD, which can contain extracted parasitics, complex semiconductor device models (such as BSIM or PSP). As such, it fully handles strong nonlinearities of any kind and is not limited to polynomials. Furthermore, in view of the fact that the PPV phase macromodel is also suited for predicting the gamut of other oscillator/PLL phenomena, the new technique is especially suited for use in comprehensive, next-generation PLL design methodologies [10].

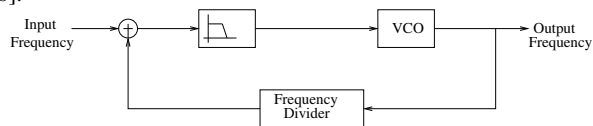


Fig. 1. PLL: Architecture of Frequency Synthesis

The remainder of the paper is organized as follows. In Section II, we provide a brief introduction to the nonlinear, PPV-based phase macromodel equation at the core of our SHIL prediction approach. In Section III, we analyse the PPV equation to develop insights into SHIL, as well as a concrete criterion for detecting SHIL in macromodel simulations. In Section IV, we apply the new technique to a standalone oscillator and an ILFD-based PLL, and provide validations/comparisons against full SPICE-level simulation.

## II. PPV EQUATION AND PHASE MACROMODEL

The first work on prediction of IL is apparently the classic work of Adler [7] in 1946; this was followed by many others. These class of methods provides intuition into LC oscillator IL mechanisms, but does not fully account for nonlinearities and higher harmonics, which limits their use to approximate analysis of restricted classes of oscillators.

The use of phase domain macromodels for oscillators is widespread in PLL design [1], [16]; however, these macromodels have not been useful, until recently, for IL related phenomena. Most available phase macromodels are based on linear integration of a perturbing input to generate output phase deviation (e.g., [17]–[22]) and are therefore provably unable to handle IL, which depends crucially on phase macromodel nonlinearity [13]. In this short section, we note the basics of the nonlinear phase macromodel [23], which we will use in prediction of super-harmonic locking in the oscillator.

Given a free-running oscillator, denote by  $x_s(t)$  its steady state (i.e., the periodic, time-domain waveforms of voltages/currents in the circuit). It can be shown that the response of the oscillator under external perturbation will be given by  $x_s(t + \alpha(t)) + y(t)$  [13], [23], where  $\alpha(t)$  is a (usually growing) phase deviation and  $y(t)$  is a small amplitude variation. The phase  $\alpha(t)$  of the perturbed oscillator can be shown to be governed by the PPV equation [23]

$$\dot{\alpha}(t) = V_1^T(t + \alpha(t)) \cdot b(t). \quad (1)$$

In (1), the quantity  $V_1(t)$ , also a periodic vector waveform with the same frequency/period as  $x_s(t)$ , is called the Perturbation Projection Vector (PPV). One of the utilities of (1) is that it is based on a rigorous and general theory, which makes it applicable to any kind of oscillator, however complex or varied. We will use the above equation in the next sections to determine techniques and criteria for superharmonic injection locking.

## III. SUPERHARMONIC IL VIA THE PPV EQUATION

In this section, we use (1) to understand SHIL and derive criteria for detecting the phenomenon. The utility of  $\alpha(t)$  for IL is that its derivative directly provides the frequency of the oscillator at any given point in time. In particular, if the perturbed oscillator becomes locked to an externally applied frequency, we are interested in determining an analytical form for  $\alpha(t)$  that reflects this condition, and in using it for predicting SHIL.

To develop intuition into IL and SHIL, consider first the simplified case where the oscillator's steady-state response is a pure sinusoid, i.e., given by  $x_s(t) = \sin(2\pi f_0 t)$ . Now we perturb this oscillator by a signal  $b(t) = A_{inj} \sin(2\pi f_1 t + \theta)$ , where  $\theta$  is a constant phase and the external signal's frequency is  $f_1$ . If  $f_1$  is almost  $M$  times of  $f_0$ , there is a possibility that the oscillator might get locked to the  $M^{th}$  sub-harmonic of  $f_1$  which would be very near to  $f_0$ , the natural frequency of the oscillator. Now suppose that oscillator has actually become locked to the  $M^{th}$  sub harmonic of  $f_1$ , i.e., the oscillator's steady state frequency is now  $\frac{f_1}{M}$ . Therefore, the oscillator new response can be given by  $x_1(t)$ , where  $x_1(t) = \sin(\frac{2\pi f_1}{M} t + \phi(t))$ .  $\phi(t)$  can, in general, be periodic with frequency  $\frac{f_1}{M}$ . The large-signal component of the new response of the oscillator (i.e., ignoring small amplitude variations) can be written as  $x_1(t) = x_s(t + \alpha(t))$ , as noted in the previous section. This implies that

$$2\pi f_0(t + \alpha(t)) = \frac{2\pi f_1}{M} t + \phi(t), \quad (2)$$

or that 
$$\alpha(t) = \left( \frac{f_1 - M f_0}{M f_0} \right) t + \frac{\phi(t)}{2\pi f_0},$$

where  $\phi(t)$  has the following form:

$$\phi(t) = \phi_{DC} + \phi_{periodic}(t). \quad (3)$$

In the above,  $\phi_{DC}$  is the DC term of  $\phi(t)$ , while  $\phi_{periodic}(t)$  is purely periodic with frequency  $\frac{f_1}{M}$  and with a zero DC component. To recapitulate, if the oscillator becomes locked to  $\frac{f_1}{M}$ , then we expect  $\alpha(t)$  to be in the form of (2) and  $\phi(t)$  to be in the form of (3). If we

differentiate (2) w.r.t time, then  $\dot{\phi}(t)$  is given as

$$\frac{\dot{\phi}(t)}{2\pi f_0} = \dot{\alpha}(t) + \left( 1 - \frac{f_1}{M f_0} \right) \quad (4)$$

Since  $\phi(t)$  is periodic with frequency  $\frac{f_1}{M}$ , so is its derivative  $\dot{\phi}(t)$ , implying that  $\dot{\alpha}(t)$  must be periodic with frequency  $\frac{f_1}{M}$ .

We emphasize here that the equations (2), (3) and (4) are valid only when oscillator is superharmonically locked, therefore, these equations are just a criterion for testing whether or not superharmonic injection locking has occurred.

Since we compute  $\dot{\alpha}(t)$  using (1), we combine (2) and (1) to obtain a more specific form for  $\dot{\alpha}(t)$  in the event of SHIL:

$$\begin{aligned} \dot{\alpha}(t) &= V_1^T(t + \alpha(t)) \cdot b(t) \\ &= V_1^T \left( \frac{f_1}{M f_0} t + \frac{\phi(t)}{2\pi f_0} \right) b(t) \end{aligned} \quad (5)$$

Since,  $V_1^T(t)$  is periodic with frequency  $f_0$ , (5) implies that  $V_1^T \left( \frac{f_1}{M f_0} t + \frac{\phi(t)}{2\pi f_0} \right)$  must be periodic with  $f_1/M$ . Also,  $b(t)$  is periodic with frequency  $f_1$ , hence  $\dot{\alpha}(t)$  becomes periodic with  $f_1/M$ , a required criterion from (4).

We can obtain graphical intuition into this change of frequency of the PPV — it is the result of squeezing/stretching of the PPV waveform along the time axis due to the phase deviation  $\alpha(t)$ . A graphical representation of this is provided in Fig. 2. For second harmonic injection locking ( $M=2$ ), the factor by which the PPV waveform will squeeze is given by  $\frac{f_1}{2f_0}$ . In the plot,  $f_1 = 2.1f_0$  was taken for illustration; therefore, the new PPV plot is squeezed by a factor of  $\frac{2.1f_0}{2f_0} = 1.05$  and thus it will now be periodic with  $f_1/2$ . For third harmonic injection locking, the PPV will need to be squeezed by the factor of  $\frac{f_1}{3f_0}$ . Another plot, where we took  $f_1 = 3.1f_0$  resulting in a squeeze factor of  $\frac{3.1f_0}{3f_0} = 1.03$  for third harmonic locking, is also shown in Fig. 2. It is obvious that if the squeeze factor is not sufficient for  $M^{th}$  harmonic locking, the oscillator will not be able to lock to the frequency  $f_1/M$ .

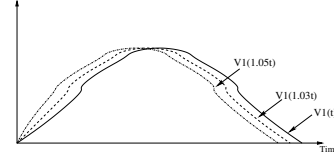


Fig. 2. Squeezing/stretching of the PPV under SHIL:  $V_1^T(t + \alpha(t))$

Our technique for predicting SHIL (or the absence of SHIL) will be to obtain  $\alpha(t)$  by numerically solving equation (1), then to compute  $\dot{\phi}(t)$  using (2). If the computed  $\dot{\phi}(t)$  has the form (3), SHIL can be confirmed by observing the slope of  $\alpha(t)$ , which should equal  $\frac{f_1 - M f_0}{M f_0}$ . In the next section, we will apply and validate this technique on standalone oscillators and PLLs, confirming that  $\phi(t)$  indeed has the form (3) when SHIL happens.

## IV. PPV-EQUATION BASED FREQUENCY-DIVIDER PLL DESIGN AND METHODOLOGY VALIDATION

### A. SHIL in cross-coupled LC Oscillator

We first simulate the cross-coupled LC oscillator circuit, shown in Fig. 3, to predict superharmonic injection locking for  $M=2$  (i.e., 2nd harmonic locking) using the above technique. Parameter values of  $l_1 = l_2 = 2.58nH$  and  $c = 5pF$  were chosen for the simulation. We used the harmonic balance method to find the oscillator's natural frequency (about 1.0009GHz) and its steady-state waveform. Following HB solution, the PPV was computed for the circuit using the technique described in [15], and using the PPV, we computed  $\dot{\alpha}(t)$  for 500 cycles by solving (1) numerically using Runge-Kutta integration, with  $b(t) = 0.0575 \sin(2\pi f_1 t)$  and  $f_1 = 2.001f_0$ .  $f_1 = 2.001f_0$  was then chosen (via a trial-and-error process) to be close enough to  $2f_0$  to excite 2nd harmonic IL. An appropriate amplitude for  $b(t)$ , about 0.0575, was similarly chosen to achieve SHIL.

The numerically computed waveform of  $\alpha(t)$  is shown in Fig. 4(a). If the oscillator is locked to  $\frac{f_1}{2}$ , then the slope of  $\alpha(t)$  should be

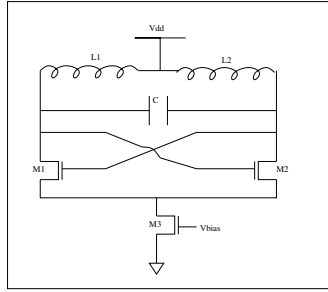


Fig. 3. Cross-Coupled LC oscillator

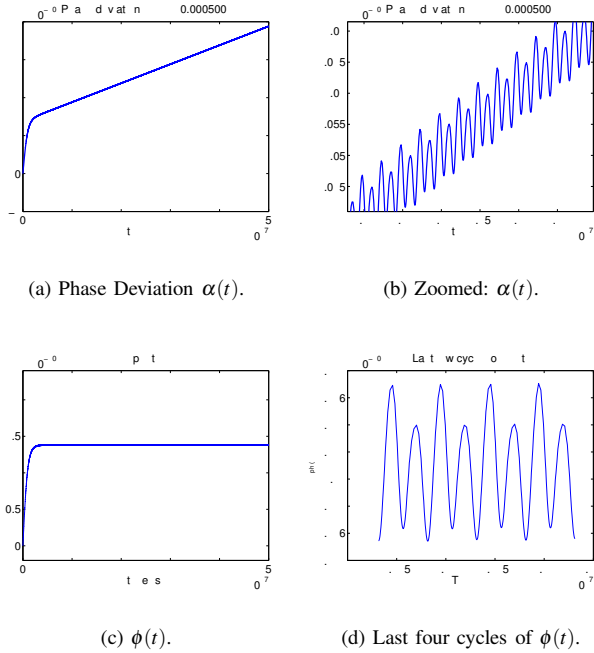


Fig. 4. M=2 SHIL (locked)

$\frac{f_1 - Mf_0}{Mf_0}$  from (2), in this case 0.005. Upon estimating the slope of the numerical  $\alpha(t)$  waveform, we confirmed a value of 0.005, implying that oscillator is indeed superharmonically locked.

More detail is available in the zoomed picture of  $\alpha(t)$ , shown in Fig. 4(b). From the zoomed version, it is clear that periodic components are present in  $\alpha(t)$ , matching our formulation (2) and further confirming presence of SHIL. We emphasize that although the correct slope of  $\alpha(t)$  is in principle sufficient to predict SHIL, we also plot  $\phi(t)$  to ensure that it is periodic in nature and of the form (3).

The plot of  $\phi(t)$  is shown in Fig. 4(c). Since the plot is for 500 cycles, we can only see the DC value of  $\phi(t)$  from Fig. 4(c). To obtain a clearer picture of the periodicity of  $\phi(t)$ , we plot the last two cycles of  $\phi(t)$  in Fig. 4(d). It can be seen from Fig. 4(d) that the waveform (four cycles) is indeed periodic, hence  $\phi(t)$  is also periodic with frequency  $f_1/2$  and also  $f_1$ . Therefore, all numerical waveforms validating our criterion for prediction of  $M = 2$  superharmonic injection locking, developed in the last section.

The above simulations were all performed using the new PPV macromodel based technique; to validate these results, we performed full simulation of the circuit. The oscillator's output voltage from full simulation is plotted in Fig. 5(a); it is evident from the plot that the oscillator is locked to  $\frac{f_1}{2}$  (in addition to measurement of the frequency of the waveforms, the absence of amplitude envelopes is a telltale indication of successful IL).

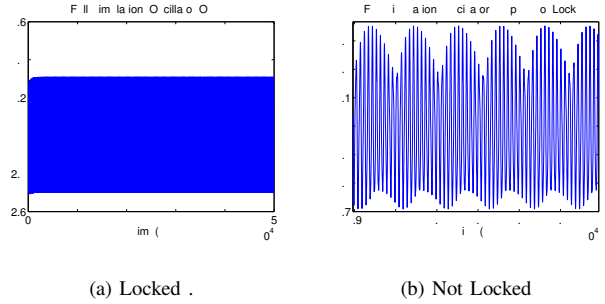


Fig. 5. Full Simulation results for locking and non-locking case

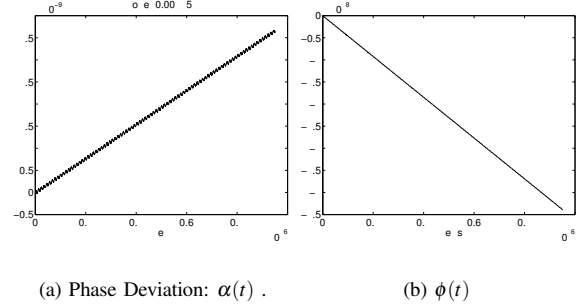


Fig. 6. For M=2; SuperHarmonic Non Injection Locking

Now, we want to simulate another case, first using the PPV macromodel and then using full simulation, where ( $M = 2$ ) superharmonic injection locking is *not* occurring. We found from various simulations that if  $b(t) = 0.08 \sin(2\pi f_1 t)$ , where  $f_1 = 2.1f_0$ , the oscillator does not lock to  $\frac{f_1}{2}$ . Plots of  $\alpha(t)$  and  $\phi(t)$  are shown in Fig. 6(a) and Fig. 6(b). In this case, the slope of  $\alpha(t)$  is 0.003856, which is not equal to  $\frac{f_1 - 2f_0}{2f_0}$ , therefore indicating the absence of injection locking. Note, also, that the plot of  $\phi(t)$  is not periodic, a consequence of the slope of  $\alpha(t)$  not being equal to  $\frac{f_1 - 2f_0}{2f_0}$ . These results are verified via full simulation. The oscillator's output voltage from full simulation is plotted in Fig. 5(b). It is clear from the plot that amplitude of the oscillator output is varying with time; closer inspection also confirms non-uniform periods, indicating that the oscillator is not locked.

We have shown, above, that the new technique is able to predict when superharmonic injection locking is occurring, as well as when it is not. It is able to do so much faster than full simulation: it took almost 3 hours to simulate 500 cycles of the oscillator using full simulation, while the new PPV macromodel based approach took about 70 seconds for 500 cycles, a speedup of about  $150\times$ .

### B. ILFD-based PLL

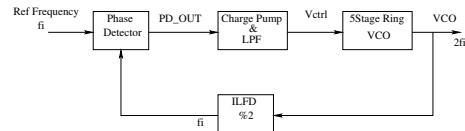


Fig. 7. PLL with ILFD

Next, we simulated/designed a PLL frequency synthesizer which incorporates a superharmonically locked oscillator as a frequency divider in its feedback path, in order to multiply its input frequency by a factor of 2. The schematic of the PLL is shown in Fig. 7. The Injection locked frequency divider (ILFD) is implemented using the cross-coupled circuit shown in Fig. 3, but its natural frequency is now changed to 100.122Mhz because the PLL which we are using

in our simulation is designed to work in the range of 80-120MHz of input reference frequency.

Note that the VCO within the PLL uses a 5-stage ring oscillator topology, with center frequency  $f_0 = 198\text{MHz}$ .  $VDD=3\text{V}$  was used for the simulation and therefore, for input frequency  $f_i = 100\text{MHz}$ , the VCO control voltage (Vctrl) (i.e., the output of the LPF block) stabilizes at 1.55V, resulting in a VCO center frequency at 198MHz (slightly less than 200MHz). The control voltage is plotted in the Fig. 8.

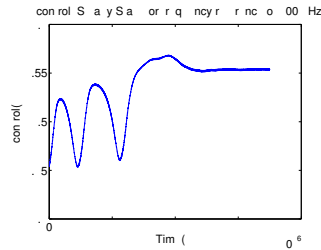


Fig. 8. Steady State of Vcontrol; steady at 1.55V for  $f_{ref} = 100\text{MHz}$

The steady state behavior of Vcontrol confirms correct working of the ILFD, i.e., the oscillator in the feedback path is getting locked to the second sub-harmonic frequency of the VCO's output frequency, thus enabling correctly-locked PLL operation. Having obtained the steady state of Vcontrol, we try to observe the unit step response of the PLL under different reference frequencies, using both full simulation of the circuit and a full-PLL macromodel (using the approach of [12]). Vcontrol waveforms from full simulation for the unit steps  $f_{ref} = 1.02f_i$  and  $f_{ref} = 1.03f_i$  are plotted in Fig. 9(a) and Fig. 9(b). It is clear from the plot that Vcontrol tracks the change in the reference frequency.

Next, we obtained the same step response using the PPV phase macromodel technique of [12], augmented with an extra nonlinear PPV macromodel for the ILFD – in other words, the PLL contains two oscillator macromodels, one for the VCO and one for the ILFD. Responses of the PLL to step changes in reference frequency are shown in Fig. 9(a) and Fig. 9(b). It is clear from the results that our nonlinear macromodel approach for the simulation of PLL exactly tracks the plots obtained from the full simulation. For  $f_{ref} = 1.02f_i$ , Vcontrol became stable at 1.61V both from full simulation and from the macromodel based simulation; for  $f_{ref} = 1.03f_i$ , Vcontrol reached 1.64V, again both from full simulation and from the macromodel.

Thus, using the PPV-based phase macromodel, we have demonstrated successful use of ILFDs as a frequency dividers in PLL and have also We can now compare the speedups that we have obtained using the macromodel. Full simulation of the PLL took about 1 hour 6 min (step response simulation of 50 cycles), while the macromodel-based approach took only 20 seconds for the same simulation – a speedup of about  $200\times$ .

## REFERENCES

- [1] K. Kundert. *Predicting the Phase Noise and Jitter of PLL-Based Frequency Synthesizers*. www.designers-guide.com, 2002.
- [2] R. Mohanavelu and P. Heydari. A novel ultra high-speed flip-flop-based frequency divider. *Circuits and Systems ISCAS 2004*, 4:169–172, May 2004.
- [3] T. S. Ayur and B. Razavi. A 2-ghz, 6mw bicmos frequency synthesizer. *IEEE Journal of Solid-State Circuits*, 30:1457–1462, December 1995.
- [4] C. G. S. Michael, H. Perrott, and T.L. Tewksbury. A 27-mw cmos fractional-n synthesizer using digital compensation for 2.5-mb/s gfsk modulation. *IEEE Journal of Solid-State Circuits*, 32:2048–2059, December 1997.
- [5] S. Verma, H.R. Rategh, and T.H. Lee. A unified model for injection-locked frequency dividers. *IEEE Journal of Solid-State Circuits*, 38(6):1015–1027, June 2003.
- [6] H.R. Rategh and T.H. Lee. Superharmonic injection-locked frequency dividers. *IEEE Journal of Solid-State Circuits*, 34:813–821, June 1999.
- [7] R. Adler. A study of locking phenomena in oscillators. *Proceedings of the I.R.E. and Waves and Electrons*, 34:351–357, June 1946.
- [8] K. Kurokawa. Injection locking of microwave solid state oscillators. *Proc. IEEE*, 61:1386–1410, October 1973.
- [9] B. Razavi. A study of injection locking and pulling in oscillators. *IEEE Journal of Solid-State Circuits*, 39(9):1415–1424, September 2004.

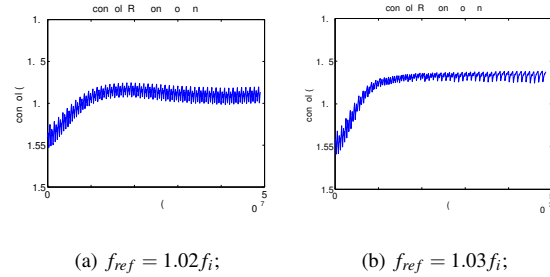


Fig. 9. Step Response of PLL: Generated Using Full Simulation;  $f_i = 100\text{MHz}$

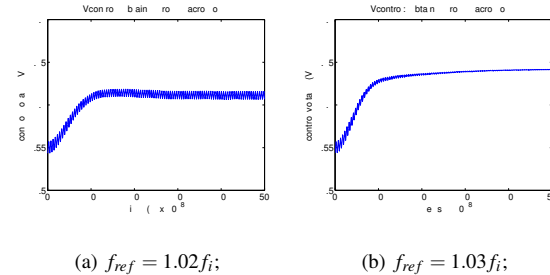


Fig. 10. Step Response of PLL: Generated Using Macromodel ;  $f_i = 100\text{MHz}$

- [10] Prashant Goyal, Xiaolue Lai, and Jaijeet Roychowdhury. A fast methodology for first-time-correct design of pll's using nonlinear phase-domain vco macromodels. *Proceedings of the 2006 conference on Asia South Pacific design automation*, pages 291–296, 2006.
- [11] T. Mei and J. Roychowdhury. Oscillator-AC: Restoring Rigour to Linearized Small-Signal Analysis of Oscillators. In *Proc. IEEE ICCAD*, pages 604–609, 2005.
- [12] X. Lai, Y. Wan, and J. Roychowdhury. Fast PLL simulation Using Nonlinear VCO Macromodels for Accurate Prediction of Jitter and Cycle-Slipping due to Loop Non-idealities and Supply Noise. *Proc. IEEE Asia South-Pacific Design Automation Conference*, January 2005.
- [13] X. Lai and J. Roychowdhury. Capturing oscillator injection locking via nonlinear phase-domain macromodels. *IEEE Trans. Microwave Theory Tech.*, 52(9):2251–2261, September 2004.
- [14] A. Demir, A. Mehrotra, and J. Roychowdhury. Phase noise in oscillators: a unifying theory and numerical methods for characterization. *IEEE Trans. on Circuits and Systems-I: Fundamental Theory and Applications*, 47(5):655–674, May 2000.
- [15] A. Demir and J. Roychowdhury. A Reliable and Efficient Procedure for Oscillator PPV Computation, with Phase Noise Macromodelling Applications. *IEEE Trans. Ckts. Syst. – I: Fund. Th. Appl.*, 2003. Accepted for publication.
- [16] J.L. Stensby. *Phase-locked loops: Theory and applications*. CRC Press, New York, 1997.
- [17] A. Demir, E. Liu, A. L. SAngiovanni-Vincentelli, and I. Vassiliou. Behavioral simulation techniques for phase/delay-locked systems. *Proceedings of the Custom Integrated Circuits Conference 1994*, pages 453–456, May 1994.
- [18] M. Gardner. *Phase-lock techniques*. New York: Wiley, 1966.
- [19] A. Hajimiri and T.H. Lee. A general theory of phase noise in electrical oscillators. *IEEE Journal of Solid-State Circuits*, 33(2), February 1998.
- [20] J. Lee, K. S. Kundert, and B. Razavi. Modelling of jitter in bang-bang clock and data recovery circuits. *Proceedings of the Custom Integrated Circuits Conference 2003*, pages 711–714, September 2003.
- [21] M. Takahasi, K. Ogawa, and K. S. Kundert. Vco jitter simulation and its comparison with measurement. *Proceedings of Design Automation Conference 1999*, pages 85–88, June 1999.
- [22] P. Vanassche, G. G. E. Gielen, and W. Sansen. Behavioral modeling of coupled harmonic oscillators. *IEEE Trans. on Computer-Aided Design*, 22:1017–1026, August 2003.
- [23] A. Demir, A. Mehrotra, and J. Roychowdhury. Phase noise in oscillators: a unifying theory and numerical methods for characterization. *IEEE Trans. Ckts. Syst. – I: Fund. Th. Appl.*, 47:655–674, May 2000.